Towards a Low-cost Portable Reader for Reflective-Mode Microwave Sensors

Mahmoud Elgeziry, Filippo Costa, *Senior Member, IEEE*, Paris Vélez, *Senior Member, IEEE*, Ferran Paredes, *Senior Member, IEEE*, Ferran Martín, *Fellow, IEEE*, and Simone Genovesi, *Senior Member, IEEE*

***Abstract*—Microwave sensors are typically characterized by using a Vector Network Analyzer (VNA) that measures the scattering parameters of the device under test (DUT) over a wide frequency band with great accuracy. However, these features of the VNA are not always required and its bulky form factor and high cost can be even a limitation in many practical scenarios such as microwave sensors, which are generally characterized by low cost, small footprint, and often planar profiles. This paper presents a novel low-cost portable reader for reflective-mode microwave sensors. The proposed device is based on a hybrid 180° directional coupler that separates the input signal from the reflected one, a Voltage Controlled Oscillator (VCO) to generate the input signal, and a Gain/Phase detector board. The performance of the proposed system has been experimentally assessed for reference load cases, showing a good match between simulated and measured results. The capability and usefulness of the proposed device is demonstrated through the implementation of a reflective-mode distance sensor where the input impedance of the one-port sensing element is the output variable of interest. The results obtained with the proposed reader well match with the VNA measurements with a mean error of about 8%. It is worth noting that the presented solution can be easily adopted as the measurement device by other reflective-mode sensors, operating in the coupler's frequency band. Overall, the proposed novel reader offers a new approach to measuring the output variable of one-port reflective-mode microwave sensors that is battery-powered, portable, versatile, accurate and cost-effective compared to using a VNA.**

***Index Terms*—microwave sensor, hybrid coupler, distance sensor, reflective-mode sensor, spiral resonator**

I. Introduction

WIRELESS microwave sensors are devices that use electromagnetic waves at microwave frequencies to detect and measure various physical quantities, including but not limited to: permittivity, temperature, pressure, humidity, composition, displacement and velocity. They are widely used in industrial, environmental, and medical applications due to their high sensitivity, accuracy, and non-destructive nature. Resonant elements inspired by metamaterial geometries such as the widely used Split Ring Resonator (SRR) and the Spiral Resonator (SR) have been extensively employed in sensing applications [1]–[4] due to their high sensitivity, miniaturization capability, high Q-factor, and their simple and inexpensive design and fabrication techniques [5]. The configuration of the sensor is the basis of an important classification of this type of microwave sensors. For example, considering a sensor configuration where the resonator is coupled to a two-port network (ex: a transmission line), the parameter of interest is, in most cases, the transmission coefficient (S_{21}) of this line, and these sensors are referred to as Transmission-mode sensors. Whereas for a resonator coupled to a one-port device (ex: antenna),the monitored parameter is usually the reflection coefficient (S_{11}) at the antenna terminals, this group of sensors is called Reflective-mode sensors. Different classifications of microwave sensors based on other parameters such as: output variable of interest (resonant frequency, amplitude of S_{11} or S_{21}, or their phases) have been thoroughly demonstrated in recent works in the literature [6]. The main focus of this work is dedicated to resonating microwave sensors due to their higher sensitivity and smaller size foot-print, and compatibility with other applications such as wearable sensors [7].

Radio frequency and microwave sensors have been commonly used for sensing the properties of the material under test (MUT) as evidenced by the increasing number of works in the literature employing dielectric permittivity sensors based on resonators inspired by metamaterials [8], [9]. The operating principle of such sensors is based on the change of the effective permittivity perceived by the sensor due to the presence of the MUT, or Liquid Under Test (LUT) in case of sensors measuring the permittivity of fluids [10], [11]. The same sensing concept was implemented for other physical parameters that influence the permittivity. For example tactile [12], water level [13], flow rate [14], ambient conditions [15], [16], air bubbles in blood stream [17], and gas [18] sensors. As a result of this change in effective permittivity seen by the sensor, the sensing principle in these devices is in most cases relying on a shift of the resonant frequency of the sensor compared to the the original unloaded case.

The broadband measurement of the shift in the resonant frequency is not a simple quantity to measure since it typically requires the use of expensive measurement instruments that perform a frequency sweep over the operating range of the sensor. As a result, techniques to simplify the required measurement have been proposed in the literature, indeed,

"This work was partially supported by the Italian Ministry of Education and Research (MIUR) in the framework of the CrossLab and Forelab projects (Departments of Excellence)."

"This work was supported by MCIN/AEI 10.13039/501100011033, Spain, through the projects PID2019-103904RB-I00 (ERDF European Union) and PDC2021-121085-I00 (European Union Next Generation EU/PRTR), by the AGAUR Research Agency, Catalonia Government, through the project 2021SGR-00192, and by Institució Catalana de Recerca i Estudis Avançats (who awarded Ferran Martín).

Mahmoud Elgeziry (mahmoud.elgeziry@phd.unipi.it), Filippo Costa (filippo.costa@unipi.it), and Simone Genovesi (simone.genovesi@unipi.it) are with the Department of Information Engineering in the University of Pisa, Pisa, 56123, Italy.

P. Vélez, F. Paredes, and F. Martín are with GEMMA/CIMITEC, Departament d'Enginyeria Electrònica, Universitat Autònoma de Barcelona, 08193 Bellaterra, Spain

sensors relying on monitoring either the amplitude or phase, of either the reflection or transmission coefficients, at a single frequency have been found in the literature. For instance a lateral displacement transmission-mode microwave sensor operating at a single frequency has been proposed in [19]. On the other hand, a sensor for dielectric characterization of solids and liquids has been presented in [20] where the measurement of the dielectric properties of liquids and solids was achieved by monitoring the magnitude of the transmission coefficient at a single frequency. A dielectric permittivity sensor based on the variation of the phase of the reflection coefficient, at a fixed frequency, with the dielectric permittivity of the MUT has been proposed in [21]. On the other hand, single-frequency sensing solutions featuring an antenna instead of a transmission line as the sensing part of the reader were also found in the literature for different applications such as: displacement [22], wearable respiration rate sensor [23], strain [24], path detection sensors for Autonomously Guided Vehicles (AGVs) [25]. The sensing principle was based on the near-field interaction between the probing antenna and an SR tag in the sensing region of the device. The sensor output was retrieved by measuring the amplitude of S_{11} at a single frequency corresponding to the resonant one. This is, indeed, a relatively simple measurement as it only requires a single-frequency one-port measurement of the magnitude of the reflection co-efficient.

The commonly used instrument for this purpose is the Vector Network Analyzer (VNA) which, indeed, has been used in each of the previously cited works employing microwave sensors. VNAs offer multiple-port measurements of the complex scattering parameters over a wide range of frequencies. Indeed, there is no doubt about the usefulness of such instrument, especially in prototyping phase as has been demonstrated in the presented solutions. However, in addition to its high cost, the use of VNAs makes almost impossible the implementation of the microwave sensor in a practical scenario due to its bulky size. Therefore, the search for alternative solutions for signal measurement and generation has received attention from the research community [26]–[29]. Especially when the required measurement of the output variable of interest does not necessarily require a sophisticated instrument such as the VNA. The solution presented in [28] allowed the detection of a finger touch on two distinct SRRs. The measurement system developed in this work relied on a commercial Voltage Controlled Oscillator (VCO) and an RF power detector chip. The authors were able to determine the state (touched or untouched) of their touch-pad using this system by linking the output voltage of the RF power detector to the transmission coefficient of the line.

In this paper, a portable low-cost reader for one-port reflective-mode resonant microwave sensors is presented. The challenge in performing the measurement relies in the fact that the sensitive part of the sensor is a one-port device; for example an antenna. For this reason, a tailored method for separation of the input and reflected signals is realised thanks to a design based on a rat-race coupler; which has proven to be an efficient and low-cost technique compared to the use of other signal separation devices such as a circulator, which would significantly increase the cost of the system. In the work presented herein, we propose a reader to retrieve the output of reflective-mode microwave sensors using a full *plug-and-play* solution made of a signal generator (a commercial VCO), A Gain/phase detector chip, and the rat-race coupler that can be connected to the sensor, operating in the coupler's frequency band, by means of a standard SMA cable. This first prototype of the reader can be used as a reliable substitute, even in proof-of-concept or characterization phase, to VNAs in microwave sensors design. This enables the development and testing of such sensors in real practical scenarios as opposed to just proof-of-concept.

Section II shows the proposed measurement system, together with the design and verification of the rat-race coupler. Section III presents the prototype of the complete portable reader, including the VCO and the gain/phase detector. The proposed sensor is implemented in a reflection-mode distance sensor based on a resonating tag inductively coupled to a microstrip loop antenna which is the sensing part of the sensor. The measurements from our proposed device are compared to measurements from a VNA in the final part of section III. Finally, the main outcomes and contributions of this work are summarised in section IV

II. Proposed Measurement System

Sensors relying on a variation of the reflection coefficient (or alternatively, the input impedance [30]) as the output variable of interest have the characteristic feature of using the same physical port for input and output signals, *i.e.*, same port for signal generation and measurement. Naturally, this requires the separation of the input and output signals to enable the measurement of the amount of reflected power at the antenna. This can be accomplished with circulators, but these components are costly and bulky. The alternative solution proposed in this paper and reported previously in [27] is based on the implementation of directional couplers, specifically 180° hybrid couplers.

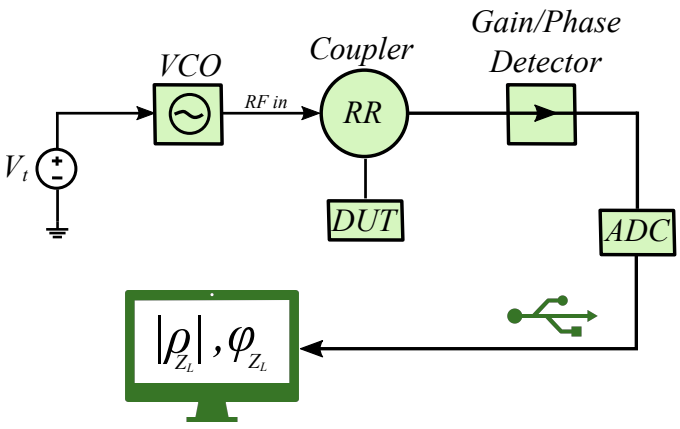

Fig. 1. Schematic flow diagram showing the setup of the proposed measurement system. The Device Under Test (DUT) is connected to the coupler and the measurement is obtained using the Gain/Phase detector

The architecture of the proposed system is depicted in Fig. 1. The input tuning voltage, V_t controls the frequency of the output signal from the Voltage Controlled Oscillator

(VCO). This signal is then input to the coupler which is connected to the Device Under Test (DUT), which represents the sensor in the final configuration. The output of the coupler is input to a Gain/Phase detector, which evaluates the magnitude and phase of the reflection coefficient of the DUT connected to the coupler. After passing through the Analog-to-Digital Converter (ADC), the results are logged and displayed on the control computer. The design of the coupler is detailed in the following section.

A. Coupler Design

This design is a development from the solution previously presented in [27] which was based on a double rat-race design. The two hybrid couplers in such design are separated by a 360° line so that it does not introduce any phase delays. The key feature of that solution is that it was designed in a way such that the ratio between the signals at the two output ports of the coupler directly provides the reflection coefficient of the DUT, referred to as ρ_{MUT} in that work, which is a quantity that could be easily measured without the VNA. The focus of the solution in [27] is dedicated to sensors whose operating principle relies on the variation of the phase of the reflection coefficient with the physical property being measured. Therefore, the addition of the second rat-race coupler served the purpose of removing any relative scaling or delay between the output signals so that they can be directly compared for the estimation of the reflection coefficient. While the solution based on the double rat-race configuration has been verified to be effective, however, one major disadvantage is the size.

Since rat-race couplers are known to have a narrow frequency band of operation, they are designed to work at the desired operating frequency band. Consequently, the size of the coupler significantly increases with a decrease in the operating frequency. Indeed, for a sensor operating in the sub-GHz range, the dimensions of this coupler becomes excessively large. The use of a high permittivity substrate can, as a matter of fact, effectively decrease the wavelength and consequently the dimensions of the circuit as has been shown in [27] with the use of the (costly) high permittivity Rogers RO3010 substrate for the sensor operating at 1 GHz. Therefore, operating at lower frequencies would dramatically increase the size, especially if low-cost substrates (such as FR-4) are used, making it more challenging to implement such planar sensors in practical applications where space constraint is an issue.

The layout of the solution proposed in this work for separating the input signal from the reflected one is shown in Fig. 2. The design is based on a single rat-race coupler, and the input signal at the operating frequency is injected at P_2, the Δ port of the of the coupler, whereas the sensor, denoted as DUT, is connected to port P_3. Ports P_1 (Σ-port) and P_4 are the two outputs from this circuit that are used to estimate the reflection coefficient, ρ_{DUT}, of the DUT (microwave sensor) connected to port P_3.

The S-parameter matrix of the hybrid coupler shown in Fig. 2 is given by [31]:

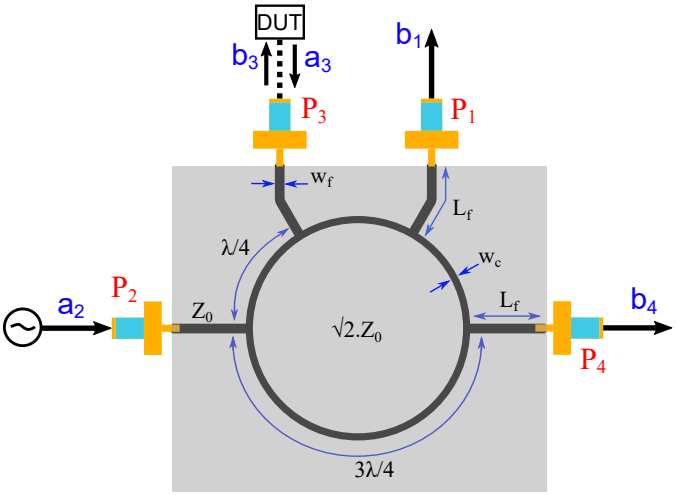

Fig. 2. Layout of the proposed rat-race coupler for separating the input from the reflected signal. a_3 represents the reflected part of the signal input to the DUT connected to port P_3 of the coupler.

$$S = \frac{-j}{\sqrt{2}} \begin{bmatrix} 0 & 0 & 1 & 1 \\ 0 & 0 & 1 & -1 \\ 1 & 1 & 0 & 0 \\ 1 & -1 & 0 & 0 \end{bmatrix} \tag{1}$$

The length of the feeding line to the ports, L_f, should be the same for all ports to avoid the introduction of any unwanted delays. At the operating frequency of the device, any fabrication tolerances on the actual length of L_f has an insignificant effect on the phase of the output. The widths, w_f and w_c, on the other hand depend on the impedances of the ports and the central ring. The impedance of the ports of the rat-race coupler are set to $Z_0 = 50\Omega$ whereas that of the ring is equal to $Z = 70.71\Omega$. Finally, the circumference of the ring is equal to 1.5 times the wavelength at the operating frequency. The reflection coefficient of the DUT, ρ_{DUT}, can be calculated using the following expressions starting from the S-matrix in (1).

$$\begin{bmatrix} b_1 \\ b_2 \\ b_3 \\ b_4 \end{bmatrix} = \frac{-j}{\sqrt{2}} \begin{bmatrix} 0 & 0 & 1 & 1 \\ 0 & 0 & 1 & -1 \\ 1 & 1 & 0 & 0 \\ 1 & -1 & 0 & 0 \end{bmatrix} \cdot \begin{bmatrix} 0 \\ a_2 \\ b_3.\rho_{DUT} \\ 0 \end{bmatrix} \tag{2}$$

from which

$$b_1 = -\frac{j}{\sqrt{2}} b_3 \rho_{DUT}. \tag{3}$$

$$b_3 = -\frac{j}{\sqrt{2}} a_2. \tag{4}$$

and combining (3) and (4), it follows that

$$S_{12} = \frac{b_1}{a_2} = -\frac{1}{2}\rho_{DUT}. \tag{5}$$

The output at port P_4 is given by

$$b_4 = \frac{j}{\sqrt{2}} a_2. \tag{6}$$

Consequently

$$S_{42} = \frac{b_4}{a_2} = \frac{j}{\sqrt{2}}. \tag{7}$$

Finally

$$\frac{S_{12}}{S_{42}} = \frac{j}{\sqrt{2}}\rho_{DUT} = \frac{b_1}{b_4} \tag{8}$$

Using this formulation, it has been demonstrated that the reflection coefficient (ρ_{DUT}) of the DUT, in this case the the sensor connected to port P_3 of the coupler, is proportional to the ratio of the outputs from the output ports (P_1 and P_4) of the coupler. Most importantly, it is a quantity that can be measured without a VNA, and can be measured by using a commercial Gain/Phase detector.

B. Design Validation

In this subsection, we present the simulation and measurement results of the proposed device, in order to validate its performance and accuracy. Supposing an operating frequency of the sensors compatible with the proposed reader ranging between 400-500 MHz, the rat-race coupler previously presented in section II-A has therefore been realised on a 1.6 mm thick FR-4 substrate ($\epsilon_r = 4.3$ and $\tan\delta = 0.03$). As a preliminary verification for this structure, it has been tested by connecting known terminations, such as: short-circuit and open-circuit loads to port P_3 of the coupler as the DUT. At the design central frequency of the coupler, 450 MHz, the circumference of the ring of the rat-race coupler is equal to 1.5 λ, and the impedance of the ring is equal to 70.71 Ω, which is equal to the port impedance (50 Ω) multiplied by $\sqrt{2}$. The design parameters of the structure are summarised in Table I

TABLE I
RAT-RACE COUPLER DESIGN PARAMETERS

Parameter	Value
Port impedance, Z_0	50 Ω
Center frequency,	450 MHz
Coupler ring circumference,	565 mm
Coupler trace width, w_c	1.56 mm
Port feeding lines length, L_f	29 mm
Port feeding trace width, w_f	3 mm

For the purpose of the verification of the structure, firstly, the reflection coefficient for these reference DUT loads has been obtained from electromagnetic simulations using Keysight PathWave Advanced Design System (ADS) 2023, which is a commercially available simulation software. The structure in Fig. 2 was modelled on the software and the DUT was added as the open circuit and short circuit terminations for comparison with the measured results. A photograph of the fabricated structure can be seen in Fig. 3 showing the SMA connectors soldered to the ports of the coupler, and an example of a loading case where the DUT is simply an open circuit termination.

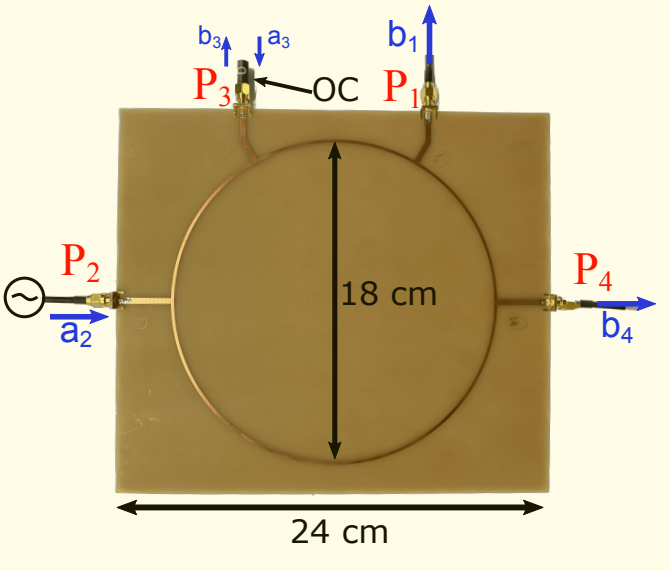

Fig. 3. Photograph of the fabricated rat-race coupler structure with an example reference load; an open circuit. b_1 and b_4 are the output signals.

The reflection coefficient of the same load cases was then measured using the VNA by measuring the expression in (8) linking the ratio between S_{12} and S_{42} to the reflection coefficient. The measured data has been post-processed to account for the length of the feeding lines L_f, connection cables, and the SMA connectors soldered on the board. Table II reports the summary of the measurements, in the form of the magnitude and phase of the reflection coefficient measured at the center frequency of 450 MHz. Finally, the magnitude and phase of the reflection coefficient of the same DUTs have been measured using the RF/Microwave Gain/Phase detector (*Model: Analog Devices AD8302* [32]) following the measurement setup described in Fig. 1. The results are also reported in Table II as $|\rho|_{AD}$ and ϕ_{AD}, respectively. These quantities are calculated by measuring the ratio between the coupler output ports (b_1 and b_4), which is proportional to the reflection coefficient as shown in (8). Fig. 4 shows the comparison between the simulation results and the measured data both using the VNA and the Gain/Phase detector for the rat-race for the case with an open-circuit termination as DUT. The VNA was chosen as a ground-truth measurement to validate the design of the rat race coupler. This is because VNAs can measure the scattering parameters (reflection and transmission coefficients) both in magnitude and phase, which is not possible using other instruments like the Spectrum Analyzer (SA) for instance. The complete characterization of the scattering parameters including phase information is crucial to the correct functionality of the proposed device

It can be observed from the figure that the good match between simulation and measurement results means that the magnitude and phase of the DUT has been accurately estimated by the proposed coupler. Moreover, the observed maximum absolute error of 0.1 and relative error of 10% in the magnitude estimation, can be attributed to losses in the real device compared to theoretical values, and 3° maximum

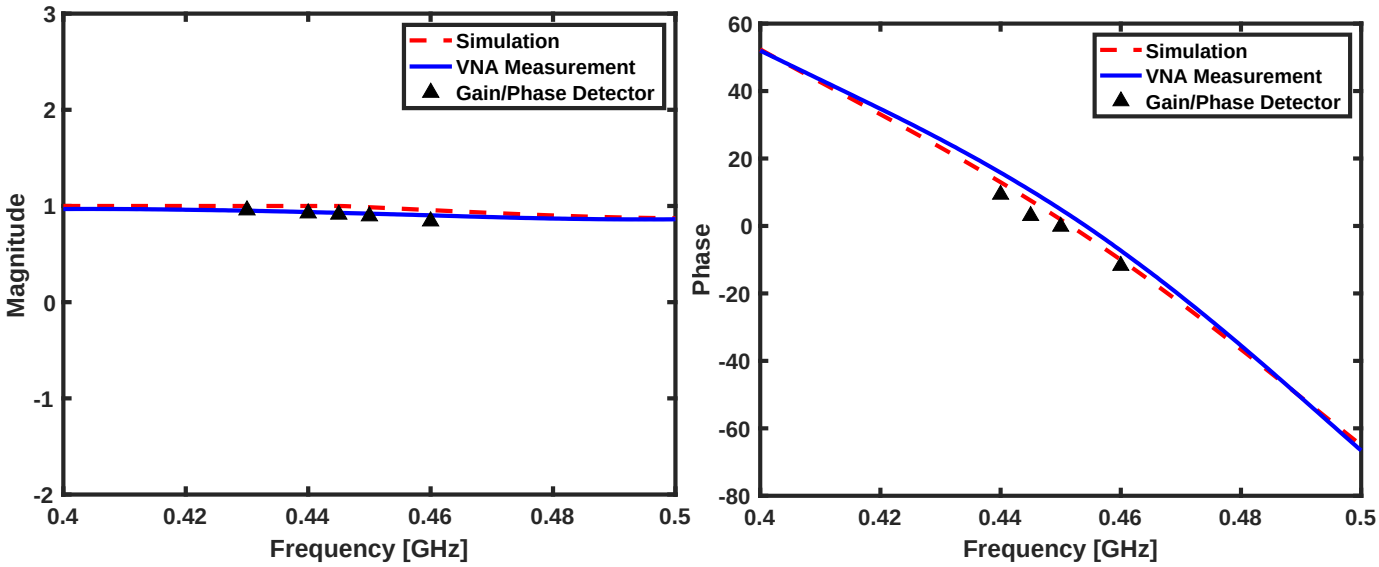

(a) Magnitude of the reflection coefficient

(b) Phase of the reflection coefficient

Fig. 4. Comparison of the value of the reflection coefficient of the open circuit termination, as DUT, for (a) magnitude and (b) phase. The results are obtained from simulations on Keysight ADS software, measurements using the VNA, and measurements using the gain/phase detector board for

absolute error (relative error = 2%) in the estimation of the phase of the reflection coefficient.

TABLE II
COMPARISON BETWEEN MEASUREMENTS OF REFERENCE LOADS AT 450 MHZ USING THE VNA AND THE GAIN/PHASE DETECTOR AND EM SIMULATIONS

	$\lvert\rho\rvert_{VNA}$	ϕ_{VNA}	$\lvert\rho\rvert_{AD}$	ϕ_{AD}	$\lvert\rho\rvert_{SIM}$	ϕ_{SIM}
OC	0.92	5°	0.90	0°	0.99	2°
SC	0.95	175°	0.91	183°	1	183°

The good agreement between the results measured using the Gain/Phase detector with the measurements from the VNA and the expected theoretical values proves the validity of the proposed portable reader for reflective-mode microwave sensors (*i.e.,* sensors relying on a change in the reflection coefficient to perform the measurement).

III. IMPLEMENTATION ON A DISTANCE SENSOR

A. SR Distance Sensor Architecture

Amplitude-modulation sensors rely on a change of the level of the coupling between the transmission line or interrogation antenna and the resonator. For the sensor presented in this section, the coupling strength between an SR tag and a microstrip probing loop antenna is modulated by changes in the distance, d_z between them as shown in Fig. 5. The sensing concept is based on linking a change in the magnitude of the real part of the input impedance of the loop antenna, Z_{in}, measured at or near to the resonance frequency, to the movement of the SR tag relative to the probe. Therefore, the SR cannot be designed independently from its probe, since the SR must be designed so that its resonance frequency is well below from the resonance frequency of the standalone probing loop antenna, and this is to avoid the interference between the resonance due to the SR and the self resonance of the probing loop.

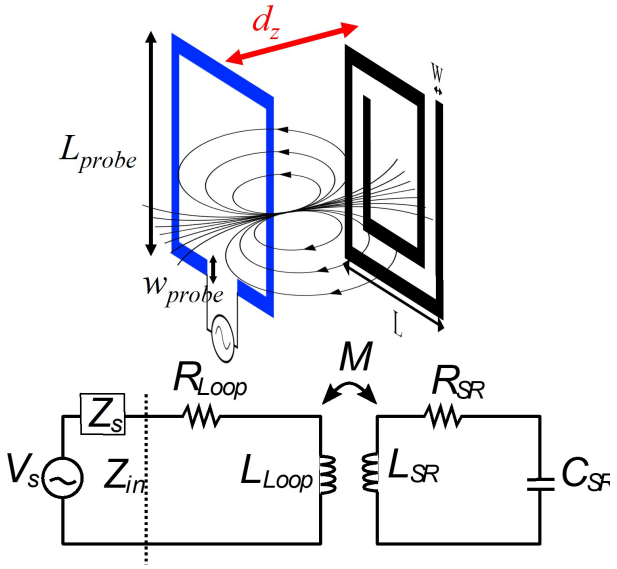

Fig. 5. Layout of the distance sensor based on a SR tag and a probing loop antenna whose output response is proportional to the distance, d_z, between them

The probing loop and the SR tag are shown in Fig. 5 where they are separated by a distance, d_z, which is the physical property of interest to be measured by this sensor. The design parameters and dimensions of the antenna and the tag are optimized so that the resonance frequency of the SR, f_{0SR} is significantly lower than that of the probe, $f_{0_{probe}}$, and according to the design guidelines presented in [33] for maximising the reading range and sensitivity. However, the design of the SR can be adapted to a different operating frequency, application, and/or desired reading range simply

by scaling up (higher reading range and smaller operating frequency) or down the dimensions of the SR as pointed out in the design guidelines.

TABLE III
SR DISTANCE SENSOR DESIGN PARAMETERS

Parameter	Value
Probe side-length, L_{probe}	30 mm
Probe Trace width, w_{probe}	2 mm
SR side-length, L	30 mm
SR Trace width, w	2 mm
SR Trace separation, s	2 mm
Number of Turns, N	1.75

The tag and probe shown in Fig. 5 were both fabricated on an FR-4 substrate ($\epsilon_r = 4.3$ $\tan\delta = 0.03$) with thickness = 1.6 mm. This is a commonly used low-cost substrate material and perfectly suitable for this application especially that the frequency of operation, in the vicinity of the resonant frequency of the SR, is kept in the sub-GHz range. The resonant frequency, f_{0SR}, of the SR is given by:

$$f_{0SR} = \frac{1}{2\pi\sqrt{L_{SR}C_{SR}}}. \tag{9}$$

where L_{SR} and C_{SR} represent the equivalent inductance and capacitance of the SR, respectively.

The values of the lumped circuit parameters (L_{SR} and C_{SR}) depend on the design parameters (L, w, s, N, and substrate material) of the SR which are reported in Table III. The external side-length of the SR, L, is set to 30 mm whereas the number of turns, N, is equal to 1.75 turns as shown in Fig. 5. The estimation of the values of the lumped parameters is not the main focus of this work and has been extensively discussed in the literature, for instance in [34]–[37]. However, The key to understanding the working principle of the sensor is analysing its equivalent circuit model shown in Fig. 5 where the SR tag is modelled using a series RLC circuit, and the strong near-field coupling with the antenna makes it possible to develop a complete circuit describing the whole system including the antenna. It is also possible to represent the components with lumped elements because they are electrically small. The strong inductive coupling between the probe and the SR tag is depends on the Mutual Inductance term, M, as previously discussed in [30]. The input impedance at resonance measured at the probing loop terminals, Z_{in}, depends on the value of the mutual inductance, which in turn is inversely proportional to d_z increases [38]. The lumped circuit parameters of the probing loop are represented by L_{Loop} and R_{Loop} in (10), whereas ω represents operating frequency. The real input impedance

$$Z_{in} = R_{Loop} + j\omega L_{Loop} + \frac{\omega^2 M^2}{j\omega L_{SR} + \frac{1}{j\omega C_{SR}} + R_{SR}}. \tag{10}$$

B. Distance Measurements

The experimental setup for measurement of distance using the SR-based sensor consists of: The SR tag which is attached to the moving platform of a linear rail (*Model: IGUS drylin*) that is actuated by means of a NEMA 23 stepper motor and a lead screw (TR10x2), and the probing loop is attached to the fixed end of the same rail. The motor is controlled using the Microcontroller Unit (*Arduino UNO board*) and is used to displace the moving cart by a known value so that the distance between the probe and the SR, d_z, changes.

Initially the VNA is employed to measure the reflection coefficient (S_{11}) at the probe terminals and is connected to the control PC through the local network and the measurements from the VNA are saved and displayed in real-time on the PC. This measurement is considered the gold standard. The conventional setup employing VNA is shown in Fig. 6. The sensor is connected to the VNA which is used to provide the input signal to the probe and to measure the reflection coefficient at the same physical input port. The measurement is performed over a narrow band and the real part of the input impedance is interrogated at the desired operating frequency, f_0, which corresponds to the resonant frequency of the SR. The measured (S_{11}) is then transformed to impedance [Ω] using the following relation:

$$Z_{in} = Z_0 \frac{1 + S_{11}}{1 - S_{11}}. \tag{11}$$

where Z_0 is the characteristic impedance of the coaxial cable. The measured data are post-processed to take into account the unbalance effect of soldering the SMA (SubMiniature version A) connector on the probing loop which is used to connect it to the VNA.

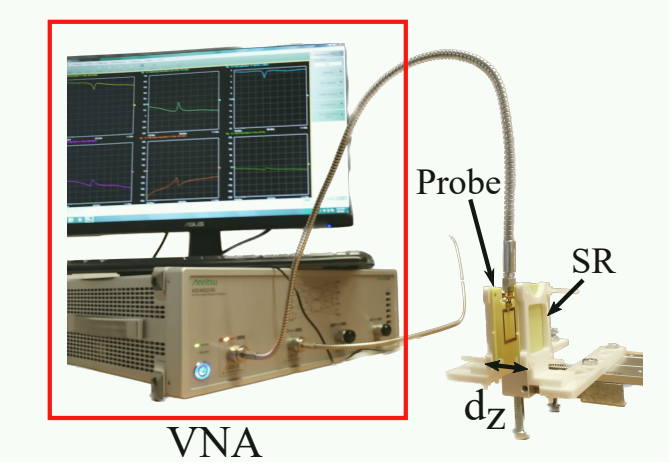

Fig. 6. Conventional experimental setup for distance measurements based on the use of VNA.

The measured real part of the input impedance is plotted against the normal distance between the probe and the tag in Fig. 8 and compared with the same result obtained from the proposed portable reader presented in the previous section.

C. Portable Reader

The proposed reader avoids the use the VNA for measuring the real part of the input impedance at the probe terminals. The measurement system using the proposed portable reader is shown in Fig. 7 along with the SR tag and probe mounted

on the testing platform, and the circuitry required to retrieve the output variable of interest. The sensitive part of the sensor (the probe) is connected to the reader by means of a coaxial cable. This represents a significant advantage since it allows the proposed device to retrieve the reflection coefficient or impedance of other DUTs or sensors connected to it via this coaxial cable connection. It is worth noting that the experimental setup for measurement using this device is the same as the one shown in Fig. 6 except that for the VNA measurement setup, the probing loop is connected to the bulky VNA as opposed to the portable reader shown in Fig. 7. The aim of this section is to show how the proposed inexpensive portable reader for reflective-mode microwave sensors allows to implement the SR-based distance sensor system at a very low cost.

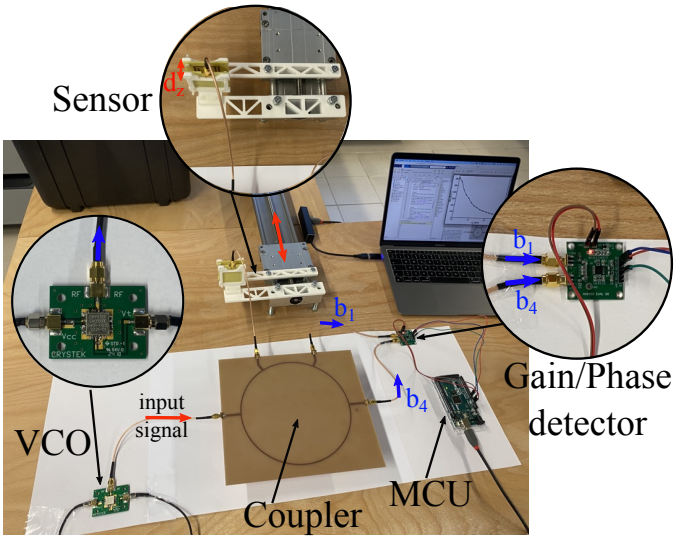

Fig. 7. Proposed portable standalone system for measuring the output variable, the real part of the input impedance, of the SR-based distance sensor.

The whole system, including the sensor and proposed reader is composed of several elements that are shown in Fig. 7. Firstly, a VCO *Model: Crystek CVCO55BE* that is used to generate the required input signal to the sensor. The VCO is controlled by the tuning voltage, V_t to produce the output signal at the desired operating frequency. The hybrid coupler previously presented and verified for separating the input signal from the output signal, the coupler output ports (Ports P_1 and P_4) are connected to the Gain/Phase Detector which measures the reflection coefficient. Finally a Micro-controller Unit (*Arduino board*) is responsible for the Analog-to-Digital Conversion (ADC) of the measured data, logging it, and providing power to the Gain/Phase detector. The input voltage to the VCO is tuned to produce the signal at 450 MHz, which is the resonance frequency of the SR tag used in this application. The Gain/Phase detector measures the magnitude ratio and phase difference of the output signals at the coupler's output ports (b_1 and b_4) of the hybrid coupler. In post-processing, that is carried out in real time, the raw measurement is corrected to account for the phase delays introduced by the addition of the coaxial cables required for connections, and the reflection coefficient is subsequently calculated following the expression in (8). The input impedance is then computed from the reflection coefficient using transmission line theory.

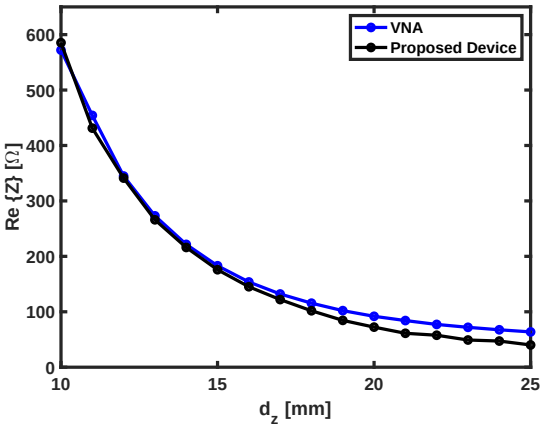

Fig. 8. Comparison between the results obtain from the VNA and those obtained from the proposed reader. The plot shows the real part of the input impedance versus the normal distance between the probe and the tag, measured at 450 MHz for both cases

The real part of the input impedance at the probing loop terminals measured using the proposed reader described in this section is shown in Fig. 8. The same measurements performed by the VNA is plotted in the same figure for comparison purposes. It can be observed from the figure that the agreement between the results measured by our proposed device and those obtained from the VNA is very good and the proposed system can be considered experimentally verified. The sensitivity of the proposed system is calculated as the ratio between the change in the real part of the input impedance and the change in the normal distance (d_z) between the probe and the SR tag. According to Fig. 8, the difference when using a VNA (where the gain/phase detector is not involved) or the proposed portable system is small, from which it can be concluded that the sensitivity is not severely affected by the gain/phase detector characteristics. The significance of the result in Fig. 8 lies in the fact that it has been shown that an accurate real-time measurement of distance can be obtained using the proposed portable measurement device. The relative error is calculated by computing the difference between the ground-truth value (VNA) measurement and the value obtained from the Gain/Phase detector and dividing it by the value of the VNA measurement, the proposed system demonstrated a percentage of average relative error below 8% in this case. It is important to note that the primary purpose of this work has not been to present an optimal sensor tailored to a particular application, but rather to validate and verify a low-cost versatile portable reader for amplitude-modulation microwave sensors while avoiding the use of costly instruments such as the VNA or Signal generators. In this particular case, the measurand of interest was the distance, however, the sensor can also be implemented in other applications where another physical parameter of interest can modulate the amplitude, for instance: Rotation, Lateral displacement, and orientation. The versatility provided by this design is emphasised in its *plug-and-play* feature thanks to its connection to the sensor (previously denoted as the *DUT*)

through a standard SMA cable. Moreover, the proposed reader for reflective-mode microwave sensors is characterized by its low cost compared to using an instrument such as the VNA. Our proposed reader is composed of two main inexpensive off-the-shelf integrated circuits (ICs): the VCO ($14) and the Gain/Phase detector ($10), amounting to a total cost of about $25. The presented cost-effective reader of course can be used for a limited operating frequency band as opposed to VNAs which have wide frequency range but also cost 2-3 orders of magnitude more. It is worth noting that the reader can be battery operated, offering full portability to the user, enabling its implementation in various sensing applications.

IV. Conclusion

A novel portable stand-alone reader for microwave sensors has been presented in this paper. The proposed devices can be used with microwave sensors whose output variable of interest is the reflection coefficient at the one-port sensing element. The design and validation of this structure have been thoroughly investigated in this work and it has been demonstrated that the reflection coefficient of the Device Under Test (DUT) can be measured using the proposed device. The reader is composed of two main parts, firstly: the 180° hybrid coupler which is used to separate the input signal from the reflected one. The functionality of this structure has been initially verified by comparing its performance for reference loads, such as an open or short circuit termination, to the expected values from theoretical analysis. The second part consists of the signal generation circuitry, by means of a VCO tuned to generate a signal at the desired operating frequency, and the Gain/Phase detector chip which is connected to the two output ports of the coupler to evaluate the reflection coefficient of the DUT. An example implementation for a one-port reflective-mode distance sensor was used to further verify the functionality of the complete reader. The distance sensor is based on a spiral resonator tag that is coupled to a microstrip probing loop which is the sensitive part of the sensor. The obtained results show that the proposed measurement system was capable of measuring the distance with a mean error of around 8% compared to the measurements from the VNA. The proposed device offers accurate measurements for one-port reflective mode sensors using a low-cost portable reader which can be used in a real-world application as opposed to using expensive and bulky laboratory instruments. In addition, this device is characterized by its versatility thanks to the connection to the DUT through an SMA cable, as opposed to other works where the sensor or DUT are a part of the reader. Future research will be focused on integrating all the system components on a single board and the miniaturization of the device.

References

[1] M. Elgeziry, F. Costa, and S. Genovesi, "Distance sensing using spiral resonators," in *2021 XXXIVth General Assembly and Scientific Symposium of the International Union of Radio Science (URSI GASS)*, 2021, pp. 1–4.

[2] A. Gharibi, F. Costa, and S. Genovesi, "Wireless sensor for precision grasping of objects and tools by robotic hands," in *2022 3rd URSI Atlantic and Asia Pacific Radio Science Meeting (AT-AP-RASC)*, 2022, pp. 1–4.

[3] A. Karami-Horestani, F. Paredes, and F. Martín, "High data density absolute electromagnetic encoders based on hybrid time/frequency domain encoding," *IEEE Sensors Journal*, vol. 22, no. 24, pp. 23 866–23 876, 2022.

[4] A. Masi, S. Rotundo, E. Canicattì, F. Molesti, D. Brizi, and A. Monorchio, "Microwave and contactless sensor for millimeter inclusions detection in biomedical applications," in *2022 16th European Conference on Antennas and Propagation (EuCAP)*, 2022, pp. 1–3.

[5] T. Chen, S. Li, and H. Sun, "Metamaterials Application in Sensing," *Sensors (Basel, Switzerland)*, vol. 12, no. 3, pp. 2742–2765, Feb. 2012.

[6] J. Muñoz-Enano, P. Vélez, M. Gil, and F. Martín, "Planar microwave resonant sensors: A review and recent developments," *Applied Sciences*, vol. 10, no. 7, 2020.

[7] M. Elgeziry, F. Costa, A. Tognetti, and S. Genovesi, "Wearable sensor for breath rate monitoring," in *2022 16th European Conference on Antennas and Propagation (EuCAP)*, 2022, pp. 1–5.

[8] A. Rivera-Lavado, A. García-Lampérez, M.-E. Jara-Galán, E. Gallo-Valverde, P. Sanz, and D. Segovia-Vargas, "Low-cost electromagnetic split-ring resonator sensor system for the petroleum industry," *Sensors*, vol. 22, no. 9, 2022. [Online]. Available: https://www.mdpi.com/1424-8220/22/9/3345

[9] J. Muñoz-Enano, P. Vélez, M. Gil, and F. Martín, "Frequency-variation sensors for permittivity measurements based on dumbbell-shaped defect ground structures (db-dgs): Analytical method and sensitivity analysis," *IEEE Sensors Journal*, vol. 22, no. 10, pp. 9378–9386, 2022.

[10] P. Vélez, C. Herrojo, X. Illa, R. Villa, J. Muñoz-Enano, L. Su, P. Casacuberta, M. Gil, and F. Martín, "A microwave microfluidic reflective-mode phase-variation sensor," in *2021 IEEE Sensors*, 2021, pp. 1–4.

[11] A. M. Albishi, S. A. Alshebeili, and O. M. Ramahi, "Three-dimensional split-ring resonators-based sensors for fluid detection," *IEEE Sensors Journal*, vol. 21, no. 7, pp. 9138–9147, 2021.

[12] S. Choi, S. Eom, M. M. Tentzeris, and S. Lim, "Inkjet-printed electromagnet-based touchpad using spiral resonators," *Journal of Microelectromechanical Systems*, vol. 25, no. 5, pp. 947–953, 2016.

[13] F. Costa, D. Brizi, S. Genovesi, A. Monorchio, G. Manara, F. Requena, and E. Perret, "Wireless detection of water level by using spiral resonators operating in sub-ghz range," in *2019 IEEE International Conference on RFID Technology and Applications (RFID-TA)*, 2019, pp. 197–200.

[14] O. Niksan, M. C. Jain, A. Shah, and M. H. Zarifi, "A nonintrusive flow rate sensor based on microwave split-ring resonators and thermal modulation," *IEEE Transactions on Microwave Theory and Techniques*, vol. 70, no. 3, pp. 1954–1963, 2022.

[15] D. N. Mahaseth, T. Islam, and U. Mittal, "Design of a microwave planar device for humidity detection," in *Sensing Technology*, N. K. Suryadevara, B. George, K. P. Jayasundera, J. K. Roy, and S. C. Mukhopadhyay, Eds. Cham: Springer International Publishing, 2022, pp. 433–441.

[16] M. Borgese, F. A. Dicandia, F. Costa, S. Genovesi, and G. Manara, "An inkjet printed chipless rfid sensor for wireless humidity monitoring," *IEEE Sensors Journal*, vol. 17, no. 15, pp. 4699–4707, 2017.

[17] A. Masi, D. Brizi, and A. Monorchio, "Millimetric inclusion detection through a contactless microwave spiral sensor for biomedical applications," *IEEE Sensors Journal*, pp. 1–1, 2023.

[18] G. Gugliandolo, K. Naishadham, G. Crupi, G. Campobello, and N. Donato, "Microwave transducers for gas sensing: A challenging and promising new frontier," *IEEE Instrumentation Measurement Magazine*, vol. 25, no. 3, pp. 42–51, 2022.

[19] A. K. Horestani, C. Fumeaux, S. F. Al-Sarawi, and D. Abbott, "Displacement sensor based on diamond-shaped tapered split ring resonator," *IEEE Sensors Journal*, vol. 13, no. 4, pp. 1153–1160, 2013.

[20] P. Vélez, J. Muñoz-Enano, A. Ebrahimi, C. Herrojo, F. Paredes, J. Scott, K. Ghorbani, and F. Martín, "Single-frequency amplitude-modulation sensor for dielectric characterization of solids and microfluidics," *IEEE Sensors Journal*, vol. 21, no. 10, pp. 12 189–12 201, 2021.

[21] P. Casacuberta, P. Vélez, J. Muñoz-Enano, L. Su, M. G. Barba, A. Ebrahimi, and F. Martín, "Circuit analysis of a coplanar waveguide (cpw) terminated with a step-impedance resonator (sir) for highly sensitive one-port permittivity sensing," *IEEE Access*, vol. 10, pp. 62 597–62 612, 2022.

[22] M. Elgeziry, F. Costa, and S. Genovesi, "Planar spiral resonators for remote tracking of displacement," in *2021 IEEE International Symposium on Antennas and Propagation and USNC-URSI Radio Science Meeting (APS/URSI)*, 2021, pp. 1357–1358.

[23] M. Elgeziry, F. Costa, A. Tognetti, and S. Genovesi, "Wearable textile-based sensor tag for breath rate measurement," *IEEE Sensors Journal*, vol. 22, no. 23, pp. 22 610–22 619, 2022.

[24] Y. Liu, M. Wang, M. Yu, B. Xia, and T. T. Ye, "Embroidered inductive strain sensor for wearable applications," in *2020 IEEE International Conference on Pervasive Computing and Communications Workshops (PerCom Workshops)*, 2020, pp. 1–6.
[25] M. Elgeziry, F. Costa, and S. Genovesi, "Radio-frequency guidance system for path-following industrial autonomous guided vehicles," in *2022 16th European Conference on Antennas and Propagation (EuCAP)*, 2022, pp. 01–05.
[26] A. Pourafzal, T. Roi-Taravella, M. Cheffena, and S. Yildirim, "A low-cost and accurate microwave sensor system for permittivity characterization," *IEEE Sensors Journal*, pp. 1–1, 2022.
[27] M. Elgeziry, F. Paredes, P. Vélez, F. Costa, S. Genovesi, and F. Martín, "A method to retrieve the output variables in reflective-mode phase-variation sensors," in *2022 52nd European Microwave Conference (EuMC)*, 2022, pp. 516–519.
[28] M. U. Memon, A. Salim, H. Jeong, and S. Lim, "Metamaterial inspired radio frequency-based touchpad sensor system," *IEEE Transactions on Instrumentation and Measurement*, vol. 69, no. 4, pp. 1344–1352, 2020.
[29] P. Vélez, F. Paredes, P. Casacuberta, M. Elgeziry, L. Su, J. Muñoz-Enano, F. Costa, S. Genovesi, and F. Martín, "Portable reflective-mode phase-variation microwave sensor based on a rat-race coupler pair and gain/phase detector for dielectric characterization," *IEEE Sensors Journal*, vol. 23, no. 6, pp. 5745–5756, 2023.
[30] M. Elgeziry, F. Costa, and S. Genovesi, "Wireless monitoring of displacement using spiral resonators," *IEEE Sensors Journal*, vol. 21, no. 16, pp. 17 838–17 845, 2021.
[31] D. Pozar, *Microwave Engineering, 4th Edition*. Wiley, 2011. [Online]. Available: https://books.google.it/books?id=JegbAAAAQBAJ
[32] "A rf/if gain and phase detector lf–2.7 ghz ad8302 - analog devices," https://www.analog.com/media/en/technical-documentation/data-sheets/ad8302.pdf, accessed: 2023-04-24.
[33] M. Elgeziry, F. Costa, and S. Genovesi, "Design guidelines for sensors based on spiral resonators," *Sensors*, vol. 22, no. 5, 2022.
[34] S. S. Mohan, M. d. M. Hershenson, S. P. Boyd, and T. H. Lee, "Simple accurate expressions for planar spiral inductances," *IEEE Journal of Solid-State Circuits*, vol. 34, no. 10, pp. 1419–1424, Oct. 1999.
[35] U. Jow and M. Ghovanloo, "Design and Optimization of Printed Spiral Coils for Efficient Transcutaneous Inductive Power Transmission," *IEEE Transactions on Biomedical Circuits and Systems*, vol. 1, no. 3, pp. 193–202, Sep. 2007.
[36] Y. Cheng and Y. Shu, "A New Analytical Calculation of the Mutual Inductance of the Coaxial Spiral Rectangular Coils," *IEEE Transactions on Magnetics*, vol. 50, no. 4, pp. 1–6, Apr. 2014.
[37] D. Brizi, N. Fontana, F. Costa, and A. Monorchio, "Accurate extraction of equivalent circuit parameters of spiral resonators for the design of metamaterials," *IEEE Transactions on Microwave Theory and Techniques*, vol. 67, no. 2, pp. 626–633, 2018.
[38] D. Ellstein, B. Wang, and K. H. Teo, "Accurate models for spiral resonators," pp. 461–464, Oct. 2012.